Integrated terahertz pulse generation and amplification in quantum cascade lasers

S. S. Dhillon,[1,a)] S. Sawallich,[1] N. Jukam,[1] D. Oustinov,[1] J. Madéo,[1] S. Barbieri,[2] P. Filloux,[2] C. Sirtori,[2] X. Marcadet,[3] and J. Tignon[1]
[1]*Laboratoire Pierre Aigrain, Ecole Normale Supérieure, UMR 8551 CNRS, UPMC Université Paris 6, 75231 Paris Cedex 05, France*
[2]*Matériaux et Phénomènes Quantiques, UMR 7162 CNRS, Université Paris VII, 75251 Paris Cedex 05, France*
[3]*Alcatel–Thales III–V Lab, Campus de Polytechnique, 91767 Palaiseau Cedex, France*

(Received 22 October 2009; accepted 12 January 2010; published online 10 February 2010)

Integrated terahertz (THz) pulse generation and amplification in a THz quantum cascade laser (QCL) is demonstrated. Intracavity THz pulses are generated by exciting the facet of the QCL with an ultrafast Ti:Sapphire laser (~100 fs) and detected using electro-optic sampling. Maximum THz field emission is found with an interband transition of 1.535 eV (809 nm) and by narrowing the excitation laser bandwidth to ~3 THz. These resonance conditions correspond to the narrowband excitation of the quantum cascade miniband, indicating that the THz pulse is generated by the photoexcited carriers that are accelerated by the applied field. The generated pulse is subsequently amplified by the narrowband gain of the laser as it propagates through the QCL cavity. © *2010 American Institute of Physics*. [doi:10.1063/1.3306733]

Terahertz (THz) pulse amplification has been recently demonstrated using THz quantum cascade lasers (QCLs),[1] where THz time domain spectroscopy (TDS) (Ref. 2) was applied to the study of QCL gain.[3,4] THz pulses are generated by an external photoconductive antenna and are coupled into the QCL via one of the device facets. The in-coupled pulse is amplified at the gain frequency and out-coupled via the opposite QCL facet. However, typically only a few percent of the input THz pulse is coupled into the device owing to mode dimensions that are comparable with the wavelengths of the THz pulse. This limits the out-coupled THz field that can be generated, which is typically smaller than the field generated by the antenna.

THz pulse generation from quantum well systems using bandgap transitions has been extensively studied[5] where electrons from the valence band are injected on ultrafast time scales into the confined conduction subbands. This can result in coherent charge oscillations between two confined subbands, Bloch oscillations or accelerated carriers through miniband transport.[6–8] This leads to a time-varying polarization that can generate electromagnetic radiation in the THz range. Since a QCL consists of a series of quantum wells and its operation based on intersubband transitions, it could act as the nonlinear medium to generate, as well as amplify, THz pulses. This would enable direct injection of the THz pulses into the amplifying region of the QCL, and avoid any external THz coupling issues.

In this letter, we demonstrate that THz pulses can be directly generated on the QCL by illuminating the QCL facet with a femtosecond near-infrared (NIR) laser. Photogenerated electrons are excited into the QCL miniband and subsequently accelerated by the applied QCL bias, which produces broad-band THz radiation. The THz pulses are then amplified by the narrowband gain of the QCL as it propagates through the waveguide.

The QCL used in this study shows laser emission at 2.1 THz. It is based on a bound-to-continuum type design that has an active region thickness of 14 μm. A single plasmon waveguide geometry was used (ridge width of 230 μm). Details on the design, processing, and performance can be found elsewhere.[4] Laser bars of cavity length 3 mm were mounted on a continuous flow helium cryostat.

Optical pulses from a mode-locked tunable 76 MHz femtosecond Ti:sapphire oscillator are focused onto the QCL facet. (The average power is 200 mW, corresponding to an average excitation density of approximately 64 kW/cm^2 assuming a spot size of diameter 20 μm). The resulting generated THz pulses propagate through the QCL cavity, exit the opposite facet and detected using free space electro-optic sampling.[3,9] The QCL is modulated with 10 μs electrical pulses at a repetition rate of 25 kHz, with the latter used as the lock-in reference for a standard balanced photodiode detection scheme.

Figure 1(a) shows the detected THz fields for various current densities applied through the QCL. Clear oscillations of the electric field are observed, that are due to THz generation at the input facet and the subsequent amplification by the QCL gain. Below the threshold current [J_{th}=86 A/cm^2 see Fig. 2(a)] the field oscillations die out quickly. As the current density (and hence the bias field) is increased toward the laser shut-off current (136 A/cm^2), longer lasting oscillations are observed, indicating a reduction in the spectral width [see Fig. 1(b)].[4] For current densities greater than 136 A/cm^2 only a few field oscillations are observed, indicating a broad spectral response of the THz pulse. The maximum detected transmitted field before laser shut-off and misalignment of the structure is of the order of 50 mV/cm. This is roughly only a factor 4 lower than that obtained after THz pulse transmission through the QCL using an antenna as an external THz source and similar excitation power.

The corresponding spectral response (Fourier transform of time scans) is shown in Fig. 1(b). All curves present a

a)Electronic mail: sukhdeep.dhillon@lpa.ens.fr.

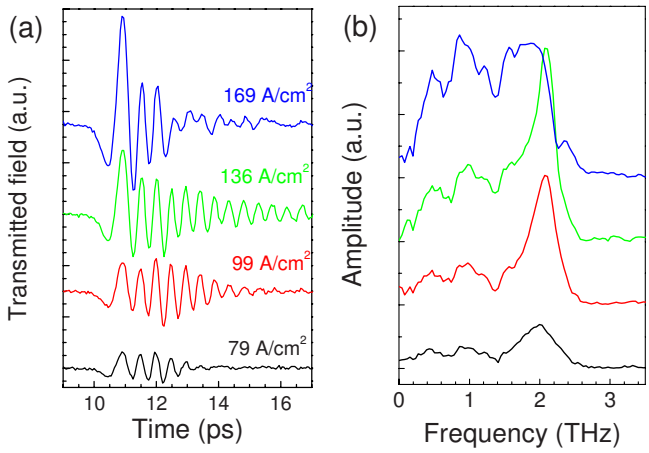

FIG. 1. (Color online) (a) Transmitted electric fields of the 2.1 THz QCL for various current densities, from below laser threshold (79 A/cm^2) to beyond laser shut-off (169 A/cm^2). (b) Corresponding spectral response (Fourier transform of the fields). Curves offset for clarity.

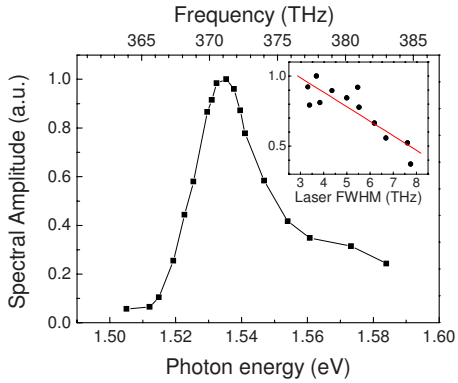

FIG. 3. (Color online) Spectral amplitude at 2.1 THz as a function of photon excitation energy of the facet excitation (laser average power is kept constant at 200 mW). A resonance is observed at a photon energy of 1.535 eV (λ=808 nm). Inset shows the spectral amplitude as a function of the linewidth of the NIR facet excitation.

broad spectral feature and, for current densities below the shut-off value, a peak centered on the frequency of the THz QCL laser emission (2.1 THz). The peak corresponds to the amplification of the pulse THz generated at the QCL facet as it propagates through the waveguide. The broad spectral response observed for current densities greater than the shut-off current is representative of the THz generated at the QCL facet *without* amplification and is further discussed below.

Figure 2(a) shows the voltage-current density (V-J) with and without NIR excitation of the QCL facet. The light output-current density (L-J) without excitation is also shown, measured using a pyroelectric detector. For a given voltage, an increase in the measured current density is observed with the NIR excitation indicating the generation of carriers into the conduction band of the QCL. In the L-J curve, laser threshold occurs at 86 A/cm^2 with maximum output power at 111 A/cm^2 and laser action totally ceasing at 136 A/cm^2. Figure 2(b) shows, as a function of current density, the spectral amplitude of the peak at 2.1 THz (filled squares) increasing rapidly as the structure aligns (>60 A/cm^2). At laser threshold, there is a sharp change in the slope and the amplitude increases linearly at a smaller rate. Laser action clamps the gain and hence should fix the pulse amplification but no clamping of the amplitude is observed in Fig. 2(b). This can be understood by considering the amplitude variation (for example) at 1.25 THz (empty squares), where there is no gain or absorption in the spectra as shown in Ref. 4. The spectral amplitude at 1.25 THz increases with current due to the increased field across the device, i.e., THz pulse generation at the facet becomes more efficient with applied bias. Therefore the unclamped behavior for 2.1 THz is a result of the increased THz generation with applied bias. Indeed, by plotting the difference in spectral amplitudes between 2.1 and 1.25 THz, we obtain the curve shown in Fig. 2(c) [A(2.1 THz)–A(1.25 THz), filled triangles] showing gain clamping at a current density of ~100 A/cm^2. The response is similar to the gain measured using externally generated pulses from a photoconductive antenna (empty circles).[4] Using the spectral amplitude at 1.25 THz as a calibration factor, the spectral gain at 2.1 THz can also be estimated from the facet excitation scheme and is shown in the inset of Fig. 2(b). A gain maximum of 10 cm^{-1} is measured at 2.1 THz, in agreement with the clamped gain in Fig. 2(c) [11 cm^{-1}, empty circles]. (A disadvantage of this method compared to previous gain studies[3,4] is that it does not use a reference at zero volts but a scan at a low applied field in the absence of amplification). A point to note is that, in Fig. 2(c), the clamping current density between the two curves is slightly different; 99 A/cm^2 for the facet generation instead of 89 A/cm^2 for the gain measurement. This indicates a small increase in the total THz losses due to the photoexcited carriers from 7.3 cm^{-1} (waveguide and mirror losses of 4 and 3.3 cm^{-1}, respectively) to 8.1 cm^{-1} with the femtosecond excitation. The optical excitation appears to only increase the losses slightly, possibly a result of a strong absorption of the former within a few microns of the QCL surface.

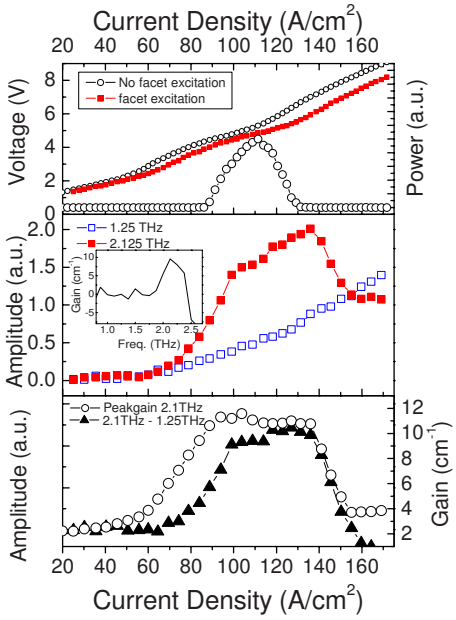

FIG. 2. (Color online) (Color online) (a) V-J curves of the 2.1 THz laser at 4.2 K with and without NIR facet excitation. The L-J is also shown without the excitation. (b) Spectral amplitude as a function of current density at the laser frequency (2.1 THz, filled squares) and at 1.25 THz (empty squares). The inset shows the calculated gain spectrum. (c) The filled triangles curve, shows the amplitude difference between the spectral amplitudes at 2.1 and 1.25 THz. For comparison, the peak gain as a function of current density measured using an external photoconductive antenna is shown.

Figure 3 shows the spectral amplitude at 2.1 THz as a

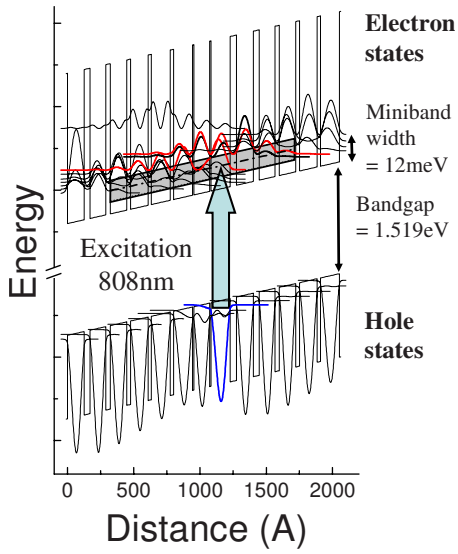

FIG. 4. (Color online) Square modulus of the electron and heavy hole wave functions at a bias of 1.8 kV/cm. The QCL electronic laser states are highlighted. The dashed line indicates the resonance wavelength (808 nm, 1.535 eV) for the spectral amplitude, corresponding to an excitation from the lowest lying hole states to the QCL miniband (large arrow). The shaded area corresponds to a bandwidth of 3 THz of the NIR laser used for the facet excitation.

function of the peak NIR energy used to excite the QCL facet. The QCL is kept at a current close to laser threshold (84 A/cm^2). At low photon energies, below the bandgap of GaAs at low temperatures (1.51 eV), no THz radiation is generated as no carriers are excited into the conduction band. As the photon energy of the NIR pulses is increased, the photons are absorbed and the spectral intensity at 2.1 THz increases rapidly and peaks at 1.535 eV before slowly decreasing as the energy is further increased. Figure 3 clearly shows a resonant behavior of the generated THz pulse, considerably different from the typical response of a photoconductive antenna.[10] The full-width at half-maximum of the curve in Fig. 3 is approximately 5 THz, corresponding to the linewidth of the Ti:sapphire laser used. Further, the inset of Fig. 3 shows the THz amplitude at 2.1 THz as a function of the linewidth of the ultrafast laser with a fixed peak wavelength of 810 nm. As the FWHM of the excitation is reduced, the spectral intensity increases monotonically. This behavior corresponds to narrowband excitation of the QCL.

These results are summarized in Fig. 4 that shows the simulated bandstructure of the QCL, illustrating both the conduction and valence bands. The THz laser transition takes place within the conduction band, between the states in bold, whereas the states in the miniband [width of approximately 12 meV (2.9 THz)] contribute essentially to transporting electrons to the following period. Due to the heavier mass, the holes are essentially confined to the quantum wells with little or no delocalization. Taking a bandgap of 1.519 eV at 4 K and a calculated hole quantization of 2.7 meV of the lowest lying state (highlighted in blue) leads to an excitation of 13.8 meV above the bottom of the conduction band for the resonant excitation of 1.535 eV illustrated previously. This is shown by the large arrow and the dashed black line. The shaded gray region corresponds to a bandwidth of 3 THz of the NIR excitation. It is clearly observed that an excitation of 1.535 eV and a bandwidth of 3 THz results in the excitation of mainly the miniband used for electronic transport. This suggests that the origin of the THz pulses generated is mainly due to charge oscillations within the miniband which has been shown to generate a broad spectral response,[7,8,11] similar to that observed for photoconductive antennas. This is supported by the observation of a photogenerated current [Fig. 2(a)] and by the fact that beyond the laser shut-off current (see Fig. 1) the THz spectral amplitude continues to increase at low frequencies and maintains a broad spectral response. Charge oscillations between the subbands involved in the laser transition seems unlikely due to the small spectral overlap of the femtosecond beam with the involved states. This would be nonetheless difficult to decouple in the current geometry from the amplification since this occurs at the same frequency.

The THz fields generated could be significantly enhanced from their current values by optimization of the cavity geometry. For example, in a regular photoconductive antenna the THz field amplitude is proportional to the applied field across the device and the latter is typically ~50 kV/cm. The applied field across the QCL during laser action is ~1.5 kV/cm. By increasing the bias field across the QCL, one increases the THz generated as shown in Figs. 1(a) and 2(b). If the bias field, however, is increased beyond the shut-off current, no amplification occurs. Decoupling the bias field on the facet from that of the QCL using a coupled cavity scheme[12] would circumvent this problem and potentially allow the bias of the QCL to be varied independently of the amplitude of the injected THz pulses from the facet. Furthermore, the facet generation technique allows the possibility of using double metal cavities for THz pulse generation and amplification, where coupling an external THz source is challenging owing to their subwavelength dimensions.

This work was financially supported by the DGA, CNano, and ANR. The LPA-ENS is a "Unité Mixte de Recherche Associée au CNRS UMR8551 et aux Universités Paris 6 et 7." The authors thank R. Feirrera for careful reading of the manuscript.

[1] R. Köhler, A. Tredicucci, F. Beltram, H. E. Beer, E. H. Linfield, A. G. Davies, R. C. Iotti, and F. Rossi, Nature (London) **417**, 156 (2002).
[2] M. Tonouchi, Nat. Photonics **1**, 97 (2007).
[3] J. Kröll, J. Darmo, S. S. Dhillon, X. Marcadet, M. Calligaro, C. Sirtori, and K. Unterrainer, Nature (London) **449**, 698 (2007).
[4] N. Jukam, S. S. Dhillon, D. Oustinov, Z.-Y. Zhao, S. Hameau, J. Tignon, S. Barbieri, A. Vasanelli, P. Filloux, C. Sirtori, and X. Marcadet, Appl. Phys. Lett. **93**, 101115 (2008).
[5] Y. Kadoya and K. Hirakawa, *Terahertz Optoelectroniques*, edited by K. Sakai (Springer, Berlin, 2005), Vol. 117.
[6] H. Roskos, M. C. Nuss, J. Shah, K. Leo, D. A. B. Miller, A. M. Fox, S. Schmitt-Rink, and K. Köhler, Phys. Rev. Lett. **68**, 2216 (1992).
[7] C. Waschke, H. G. Roskos, R. Schwedler, K. Leo, H. Kurz, and K. Köhler, Phys. Rev. Lett. **70**, 3319 (1993).
[8] Y. Shimada, K. Hirakawa, and S.-W. Lee, Appl. Phys. Lett. **81**, 1642 (2002).
[9] N. Jukam, S. S. Dhillon, Z. Y. Zhao, G. Duerr, J. Armijo, N. Sirmons, S. Hameau, S. Barbieri, P. Filloux, C. Sirtori, X. Marcadet, and J. Tignon, IEEE J. Sel. Top. Quantum Electron. **14**, 436 (2008).
[10] X.-C. Zhang, Y. Jin, K. Ware, X. F. Ma, A. Rice, D. Bliss, J. Larkin, and M. Alexander, Appl. Phys. Lett. **64**, 622 (1994).
[11] Y. Shimada, K. Hirakawa, and S.-W. Lee, Appl. Phys. Lett. **84**, 4926 (2004).
[12] S. Barbieri, C. Sirtori, H. Page, M. Beck, J. Faist, and J. Nagle, IEEE J. Quantum Electron. **36**, 736 (2000).